TOPICAL REVIEW

Magnetic properties of fullerene superconductors

V Buntar and H W Weber

Atominstitut der Österreichischen Universitäten, Schüttelstrasse 115, A-1020 Wien, Austria

Abstract. A review of the superconducting magnetic properties of doped fullerenes is presented. Experimental results on the main superconducting properties, such as the critical fields and the characteristic lengths, are critically discussed. Different methods to evaluate the lower critical field are discussed. Finally, experimental data on properties connected to flux pinning, such as the critical current density, the irreversibility line and the pinning force, are summarized and discussed.

1. Introduction

Only 10 years have passed since the fullerenes, a new type of solid carbon, were discovered [1]. During this very short time they have become one of the most fascinating and rapidly developing areas of modern science. More than a thousand publications on fullerene chemistry, physics and biology have appeared in scientific journals each year since 1990. Special journal issues [2–6] and a special monthly journal, *Fullerene Science and Technology*, are devoted to this subject. One can find several books and reviews on the chemical, physical and structural properties of these substances [7–17] and, particularly, on fullerene superconductivity [18–21]. The latter papers overview the subject of fullerene superconductivity as a whole and do not discuss all areas in detail, particularly not the magnetic properties of fullerene superconductors. Only one brief review [22] exists to date which briefly discusses some of the magnetic features of these materials. However, because of the large number of experimental results obtained by different methods on samples of different stoichiometry and quality, it is worthwhile to summarize our knowledge of this field at the present stage.

This review is organized as follows. In the introduction we discuss some of the most important and, from our point of view, the most interesting properties of the fullerene solid. In section 2 we will show some results on the main superconducting and normal state features. An enormous number of results on fullerene superconductivity is being discovered every day and even during the writing of this review. It is almost impossible to review all of them. Therefore, we will restrict ourselves to the magnetic properties of fullerene superconductors and keep the discussion in section 2 brief. Very detailed discussions of these properties can be found in the reviews by Gelfand [20] and Dresselhaus *et al* [21]. After presenting typical

results of magnetization curves in section 3, the evaluation of the critical fields and the characteristic lengths will be discussed in section 4. Superconducting properties which are connected to pinning, such as critical current density, the irreversibility line and pinning force, will be discussed in section 5. Finally, a summary of the present experimental situation will be given in section 6.

1.1. Background of fullerenes

Using a laser evaporation technique Rohlfing *et al* [23] showed in 1984, for the first time, that carbon clusters C_n with a large number of atoms (up to $n = 190$) could be produced. Mass spectrometry [23] indicated that the peaks of C_n clusters with n from 40 to 190 were not very strong and were of roughly equal peak height. Shortly afterwards, Kroto *et al* [1] demonstrated that the C_{60} peak could be increased by a factor of 40 compared to the neighbouring mass peaks by increasing the time between evaporation and expansion and by increasing the helium pressure during the laser pulse. The authors suggested that C_{60} was the most stable cluster, which consisted of 20 hexagons and 12 pentagons and had a shape very similar to the shape of a soccer ball. In honour of the architect Buckminster Fuller, who built similar structures consisting of pentagons and hexagons, the so-called 'geodesic domes', the C_n clusters were called 'buckminsterfullerenes' and as soon as it became obvious that C_{60} was only a member of a family the term 'fullerene' was used to describe them. At that time, they were considered to be an exotic species of material. Five years later, Krätschmer *et al* [24] discovered a method to separate fullerenes from carbon in the experimentally obtained carbon soot. This work showed an easy way to obtain sufficient quantities of fullerenes for experiments and led to intensive investigations of this new (fourth) form of solid carbon.

During the last 6 years, fullerenes have attracted interest from scientists in different areas such as chemistry, physics and biology. From the point of view of solid state physics, pure fullerenes and fullerene based compounds are interesting because of their molecular structure and their intriguing structural, dynamic (see for instance [14, 25–35]), magnetic [36–40] and electronic properties in the solid state [14].

C_{60} related materials have been shown to exhibit many interesting solid state properties including ferromagnetism [41–53], photoconductivity [54] and non-linear optical behaviour [55].

1.2. Solid state properties

The thermal behaviour of solid C_{60} has been reviewed in [14], [25] and [26]. At room temperature solid C_{60} has a face centred cubic (f.c.c.) crystal structure. The molecules are in complete orientational disorder and form a 'plastic crystal' [27–29]. With decreasing temperature the system undergoes a first-order transition to a simple cubic (s.c.) crystal structure at $T \sim 260$ K [28, 30]. The transition is due to the orientational re-ordering of the C_{60} molecules, although significant disorder persists to low temperatures [31, 33]. The population of the dominant orientation increases with decreasing temperature down to $T \sim 90$ K, where 83.3% of the molecules are in the dominant orientation. This occupancy does not change at lower temperatures [31].

At this temperature a glass transition was predicted theoretically [56] and anomalies were observed experimentally by neutron diffraction [31], sound velocity [57], dielectric constant [58], high-resolution dilatometry [59], specific heat [60] and other measurements. Arguments were presented [59–61] that this transition would lead to a frozen glass state. At this temperature a very interesting magnetic behaviour was observed in iodine doped C_{60} [62–65]. Buntar et al [62] performed detailed measurements of this compound at low temperatures and showed that the magnetic phenomena were due to a transition into a frozen magnetic state.

Unlike the spheroidal shape of the C_{60} molecule, the C_{70} molecule has an ellipsoidal shape. This results in an additional degree of freedom for 'packing' the solid and implies that the orientational ordering of the oblong C_{70} solid is much more complex. Vaughan et al [66] reported hexagonal close packed (h.c.p.) and f.c.c. structures for C_{70} crystals. Fleming et al [67] also reported f.c.c. and monoclinic phases. Verheijen et al [68] found four types of structure: f.c.c. at high temperature, rhombohedral (rh), ideal h.c.p. and deformed h.c.p. around room temperature. Several groups also reported on similar structures [69–72]. It is well accepted now that the thermodynamically stable form of sublimed C_{70} is the c.c.p. one (see for instance [73] for an early reference).

1.3. AC_{60} polymers

Recently, $A_x C_{60}$ systems with $x = 1$ became attractive because of their unusual structural, magnetic and electrical properties. They were first identified from a Raman analysis of the potassium compound [74]. From x-ray structural investigations the compound was found to have an f.c.c. lattice with a rocksalt structure, where the potassium ions are located on the octahedral interstitial lattice sites [75].

The alkali fulleride RbC_{60} has a number of stable and metastable modifications. Above 370 K, an f.c.c. rocksalt structure is formed [75, 76]. An orthorhombic phase [77–80] is stable below 370 K. The structure was suggested to consist of polymeric C_{60} chains, in which the individual cages were connected by a $2 + 2$ cyclo-addition along the f.c.c. unit cell. This polymerization process is stereochemically similar to the photopolymerization of C_{60} suggested by Rao et al [81]. Evidence for its polymeric character was obtained from a detailed x-ray investigation, which resulted in the unusually short C_{60}–C_{60} distance of 0.912 nm along the [110] direction of the original f.c.c. lattice [78]. Electron spin resonance (ESR) experiments [82] provided convincing evidence for the metallic nature of polymeric RbC_{60}, in which the spin relaxation is governed by electron–photon scattering, at least between the f.c.c.–orthorhombic phase transition at 410 K [77] and another transition around 50 K [76], which was claimed to be a transition into a spin density wave state. However, several μSR studies [83–86] are consistent with a disordered magnetic phase and not with long-range spin density wave order. This magnetic transition is accompanied by a metal–insulator transition [87]. CsC_{60} was found to behave similarly to RbC_{60} in this respect, but KC_{60} was recently claimed to be metallic down to very low temperatures [87].

Metastable phases of monomer C_{60}^- ions or $(C_{60}^-)_2$ dimers were formed by quenching the samples from high temperature to below 300 K [88–91]. Various phase transitions between these phases were reported [92]. Deep quenching of CsC_{60} and RbC_{60} leads to a metallic monomer phase [93] whose structure has been found to be primitive cubic ($Pa3$) by high-resolution powder neutron diffraction [94]. This is the only cubic phase of a binary C_{60} salt with a stoichiometry different from $A_3 C_{60}$ that is metallic.

2. Superconductivity of fullerenes

2.1. Background of fullerene superconductivity

Superconductivity in graphite intercalation compounds has been known since 1965, when Hannay et al [95] reported transition temperatures in alkali metal graphite intercalation compounds up to 0.55 K for C_8Cs. In the past few years, the application of a high-pressure synthesis allowed the preparation of samples with higher concentrations of alkali metals and resulted in binary graphite intercalated compounds with superconducting transition temperatures as high as 3 K in C_3K and 5 K in C_2Na. Another interesting class of superconducting graphite intercalated compounds, e.g. $C_4KTl_{1.5}$ ($T_c = 2.56$–2.7 K), becomes also superconducting as 'second-stage compounds' such as $C_8KTl_{1.5}$ ($T_c = 1.3$–2.45 K).

Conductivity [96] and superconductivity [97, 98] of the alkali metal doped fullerenes were discovered less than 1 year after the production method for bulk quantities of

C_{60} and C_{70} had been published [24]. The phenomenon of superconductivity is one of the most fascinating properties of 'the roundest of all round molecules' [10], which attracted enormous scientific interest in this new form of carbon. In many aspects the situation was similar to that shortly after the discovery of superconductivity at high temperatures in the copper oxides [99, 100]. Fullerene superconductors were the second group of materials, besides the cuprates, which overcame the previous boundary for the critical temperature, $T_c = 23.2$ K (Nb_3Ge), in conventional superconductors. More than 20 superconducting compounds of doped fullerenes have been synthesized now. The highest critical temperature ($T_c = 33$ K) occurs in the fullerene $RbCs_2C_{60}$ [101]. (Palstra *et al* [102] reported on superconductivity in Cs_3C_{60} with $T_c = 40$ K at high pressure. However, this result has not yet been reproduced). These new superconducting compounds can be prepared easily by heating alkali metal–C_{60} mixtures at $T \sim 300\,°C$ or by keeping C_{60} in an alkali metal vapour atmosphere. However, to get from the synthesis of individual samples to practical applications of these superconductors, numerous investigations of the physical properties, stability, reproducibility and elaboration of technologies for the production of large quantities for technical use are required. One of the biggest problems is their instability against air. It is enough to expose the material to air for a fraction of a second to completely destroy superconductivity. However, we believe that this main barrier can be overcome and that a knowledge of all of the superconducting parameters is the most important goal at the moment.

Numerous experimental investigations of these super-conductors, both in granular and in crystalline form, show unique properties and distinguish them from other super-conducting materials. It has been shown (see for instance [103]) that superconductivity in alkali metal doped fullerenes occurs in the f.c.c. crystal phase with the composition $A_xB_{3-x}C_{60}$ [104]. Other crystalline phases, such as body centred cubic (b.c.c.) and body centred tetragonal (b.c.t.), do not show superconductivity. In the other family of fullerene superconductors, i.e. alkali earth doped C_{60}, superconductivity occurs in simple cubic Ca_5C_{60} [105] and in b.c.c. Sr_6C_{60} [103] and Ba_6C_{60} [106]. (An additional phase, possibly Ba_4C_{60}, was found from x-ray diffractometry and there is some evidence [107] that this phase could be responsible for the occurrence of superconductivity in Ba compounds).

One of the most important results is the experimentally established empirical linear correlation of the transition temperature T_c both with the lattice constant of the cubic structure a [104, 108, 109, 101] and with the density of states at the Fermi level [110–112]. The slope of this linear $T_c(a)$ relation depends on the different structural types [113–115]. Very recently [116], a second much steeper $T_c(a)$ dependence was found for the space group $Pa\bar{3}$ [117], which could lead to much higher T_c values, if only a slightly increase in a could be achieved (figure 1). Also, it is worth stating that, as shown in figure 1, there is a different behaviour between ambient-pressure (solid line) and high-pressure (dotted line) data, unlike the case of the f.c.c. superconductors where the two sets of data coincide.
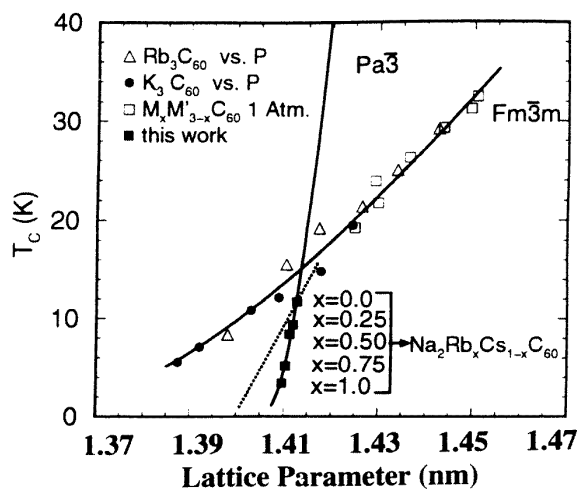

Figure 1. T_c versus a for $Fm3m$ [109, 101] and $Pa3$ ordered superconductors [117]. Solid and dashed lines are fits to McMillan's formula using linear and power law dependences, respectively, of $N(E_F)$ on the intermolecular distance; only the parameters describing $N(E_F)$ against a differ in the fits for the two families of materials. The slope of the $Pa3$ curve is much larger than that for $Fm3m$, indicating that a small increase of a without destroying $Pa3$ ordering should cause T_c to increase very rapidly. The dotted line represents the results of [212]. (After [117]).

2.2. Normal state properties

Doping C_{60} with alkali metals leads to a change of its electrical resistivity from very high values (10^8–10^{10} Ω cm for C_{60}) to a metallic-like behaviour in A_xC_{60}, because the doping results in a charge transfer to the C_{60} molecules and strongly increases the π–π overlap between them, enhancing the electrical conductivity. The electrical resistivity ρ approaches a minimum at $x = 3$, where ρ reaches typical values for high-resistivity metals [118, 119]. The low electrical conductivity can be explained by the relatively weak overlap of the electron wavefunctions between the adjacent C_{60}^{3-} ions and by the merohedral disorder in the alignment of adjacent C_{60}^{3-} ions.

Xiang *et al* [120] measured the resistivity of single-crystal K_3C_{60} and obtained a metallic behaviour $\rho(T)$ between 20 and 300 K, with a residual resistivity of 2.5 mΩ cm. Hebard *et al* [121] reported on measurements of the resistivity $\rho(T)$ for both K_3C_{60} and Rb_3C_{60} thin films. The results revealed a metallic behaviour up to 520 K without any evidence for saturation and a linear temperature dependence of the resistivity above 300 K. For Rb_3C_{60} they found that the residual resistivity was about 1.1 mΩ cm, which is less than that reported in [120]. Based on a spherical Fermi surface and on the transitional Bloch–Boltzmann approximation, the authors obtained a transport scattering length of $l_{tr} = 0.063$ nm, calculated from $\rho(520\ K) = 5.5$ mΩ cm, which is significantly shorter than the nearest-neighbour distance between the C_{60} molecules (1 nm) and the average separation of 0.6 nm between the conduction electrons, and even shorter than the distance between neighbouring C atoms in each C_{60} molecule (0.14 nm). Even for the residual resistivity
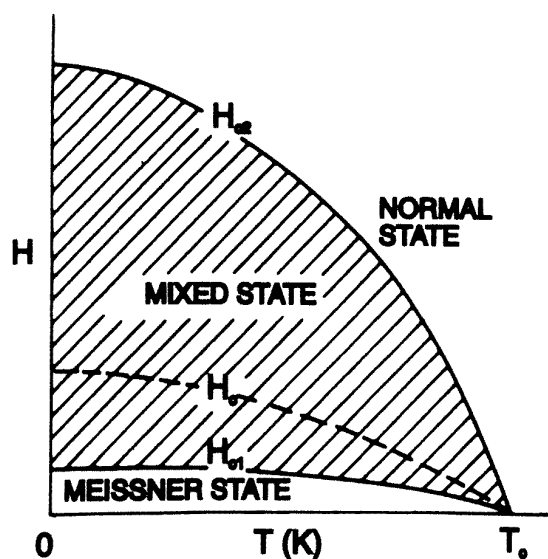
(a)
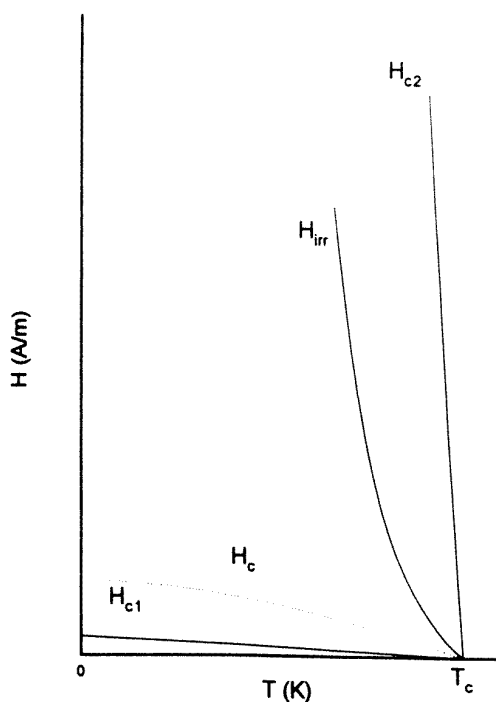
(b)

Figure 2. The magnetic phase diagram of (a) conventional type II superconductors and (b) fullerene superconductors.

Figure 3. The temperature dependence of the zero-field cooled (ZFC) and field cooled (FC) dc magnetic susceptibility of K_3C_{60} (a) crystal and (b) powder at $\mu_0 H = 1$ mT. ((b) after [131]).

constant sample volume the normal state resistivity of Rb_3C_{60} has a linear temperature dependence, $\rho \sim T$, in sharp contrast to $\rho \sim T^2$ observed under conditions of constant sample pressure. This result is important because positive $\delta\rho(T)/\delta T$ is consistent with metallic behaviour and the linear term in the temperature dependence of $\rho(T)$ is consistent with an electron-phonon scattering mechanism.

Measurements of the magnetic susceptibility χ in the normal state by Ramirez et al [111] and by Wong et al [123] demonstrated that the susceptibility was positive. $\chi(T)$ was found to be temperature independent, consistent with metallic Pauli susceptibility.

More results and discussions of the normal state scattering mechanisms can be found in [20], [21] and [124–129].

3. Magnetization curves

The first experiments on K_3C_{60} [130] and Rb_3C_{60} [131, 132] established that alkali doped fullerenes were 'strong' type-II superconductors and that their main superconducting parameters, the Ginzburg–Landau parameter κ, the penetration depth λ, the coherence length ξ and the critical fields H_{c1} and H_{c2}, were very similar to those of the high-T_c oxides.

If a type-II superconductor is subjected to a small magnetic field $H < H_{c1}$, the field is completely expelled. Shielding currents, which flow in the surface of the

(1.1 mΩ cm) we still obtain $l_{tr} = 0.3$ nm, which is too short. All this seems to indicate that the electron is for the most part confined within the surface of a given molecule before hopping to the next one. In addition, the transport electron–phonon coupling constant, λ_{tr}, was estimated in [121] and found to be $\lambda_{tr} = 4.4$ for Rb_3C_{60}, i.e. clearly strong coupling. Both of these results, a short l_{tr} and strong electron–phonon coupling, indicate predominant intramolecular electron–phonon interaction.
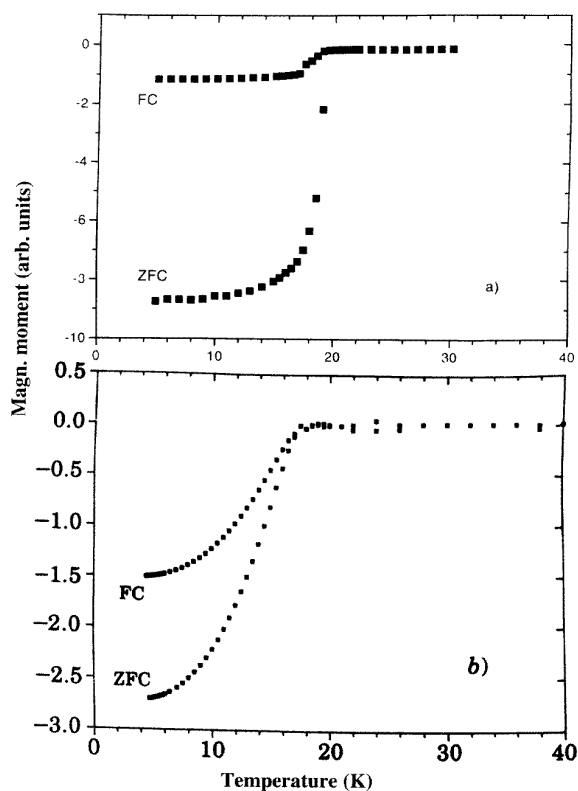
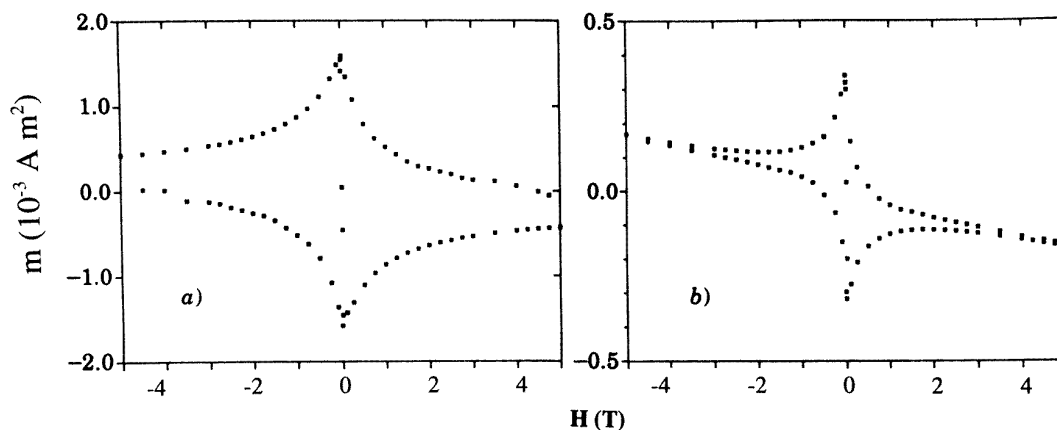Vareka et al [122] found that under conditions of

Figure 4. Hysteresis loops for Rb_3C_{60} powder at (a) $T = 7$ K and (b) $T = 20$ K (from [131]).

superconductor, prevent any penetration of flux. The superconductor is in the Meissner state and behaves like a type-I superconductor. When increasing the external magnetic field beyond the lower critical field H_{c1}, flux penetrates the sample in the form of quantized flux lines (vortices). This happens when the vortex energy is smaller than the magnetic energy associated with the current flow shielding the superconductor. The superconductor is in the mixed state, also called the Shubnikov phase. At $H > H_{c2}$, the induction B inside the sample is equal to the external field H and superconductivity is completely destroyed. Type-II superconductors in the mixed state ($H_{c1} < H < H_{c2}$) are no longer ideal diamagnets.

The magnetic field–temperature (H–T) diagram provides us with information on the main characteristic lengths, which can be calculated from the critical fields. Fullerene superconductors have, in principle, the same magnetic phase diagram as conventional type-II superconductors (figures 2(a) and (b)). However, fullerenes as well as high-temperature superconductors have an additional line between the lower and the upper critical fields, the irreversibility line $H_{irr}(T)$ (figure 2(b)). This line separates the region where the magnetization M is reversible ($H > H_{irr}$) from the region where hysteretic effects are significant. Both the critical current density J_c and H_{irr} strongly depend on flux pinning.

Measurements of the magnetization in the superconducting state are usually quite straightforward and convenient for characterizing new materials, especially powders, small crystals, fragile materials, etc, because they do not require contacts. Typical temperature and magnetic field dependences as well as the time relaxation of the magnetization M, measured on K_3C_{60} and Rb_3C_{60} superconductors [131] with a SQUID magnetometer, are shown in figures 3 and 4 and the inset of figure 5.

To obtain the temperature dependence of the magnetization (figure 3), the experiments are made as follows. The samples are cooled down to $T = 5$ K in zero external magnetic field. After temperature stabilization, a magnetic field ($\mu_0 H = 1$ mT) is applied and the magnetization monitored at increasing temperatures up to $T > T_c$. This measurement

shows the shielding fraction of the sample and is called the zero-field cooled (ZFC) curve. Then the measurement is continued at the same external magnetic field with decreasing temperature down to $T = 5$ K. This is the field cooled (FC) curve, which shows the Meissner effect. We wish to point out that the ZFC magnetization shows the flux exclusion from the sample, while the FC magnetization shows the flux expulsion. A big difference between the ZFC and FC curves (figure 3) and a strong hysteresis in the magnetic field dependence of the magnetization at fixed temperature (figure 4) indicate pinning of the magnetic vortices. The fact that the FC signal of the K_3C_{60} crystal (figure 3(a)) is very small and lies close to the zero-magnetization line shows that pinning in the sample is extremely strong and that there is almost no expulsion of the magnetic field.

The magnitudes of the ZFC and FC magnetization at the lowest temperature can be used for an evaluation of the 'superconducting fraction' X_{sc}. Indeed, the zero-field cooled susceptibility of a perfect superconductor should approach -1 at applied fields below the lower critical field. The Meissner effect for a perfect superconductor is shown schematically in figure 6(a). Then, the relation $\chi_{exp} \times 100\%$, where χ_{exp} is the experimentally obtained susceptibility, should yield X_{sc} in per cent. However, one should remember that the ZFC susceptibility does not actually represent the superconducting fraction, but the shielding fraction. For example, if the inner part of the superconductor is not superconducting and if there is only a thin superconducting surface layer, then ZFC will exhibit full flux exclusion as for a perfect diamagnet. This is shown in figure 6(b). This effect increases the effective 'superconducting fraction'. On the other hand, for powdered samples with an average grain size r, which is of the order of or slightly bigger than the penetration depth λ, flux penetrates the grains even at very small fields and this effect decreases the effective superconducting fraction (see figure 6(c)). The latter is especially important for powdered fullerene samples, which usually have $r \sim 1$ μm and $\lambda \sim 300$ nm. The influence of granularity was discussed by Baenitz et al [133, 134]. The dependence of
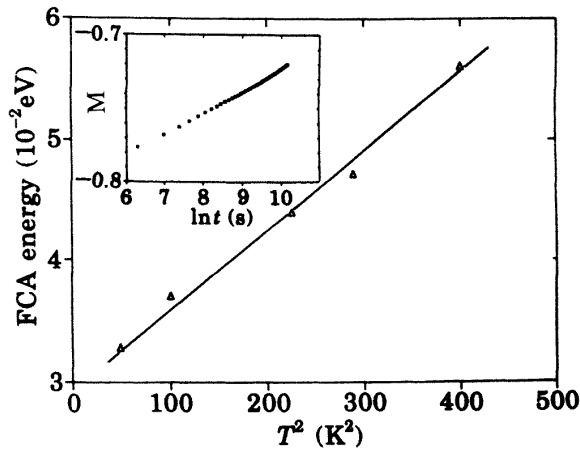
Figure 5. Flux creep activation energy (FCA) against T^2 for Rb_3C_{60} powder at $\mu_0 H = 1$ T. Inset, an example of the time decay of the magnetization at $\mu_0 H = 1$ T, $T = 7$ K. (From [131]).

the diamagnetic response on the ratio r/λ complicates the determination of the superconducting volume fraction.

In contrast to the ZFC case, field cooled curves start with the flux uniformly distributed in the sample above T_c and will show the Meissner effect at a certain temperature. This effect is masked by pinning in the system and can become almost zero in cases where pinning is very strong (see for instance figure 3(a)). This means that the FC susceptibility reveals the real X_{sc} only in the ideal case of a perfect superconductor without structural defects, i.e. without pinning centres.

This implies that the evaluation of the superconducting fraction from the ZFC and FC curves is not correct. However, there is one further way to evaluate X_{sc}, i.e. from the slope of the linear dependence of M on H at $H < H_{c1}$. This method was used in [135] and [136] and appears to be better than the others. In this work, the shielding fraction X_{sh}, which has then to be corrected by λ/r (see the next paragraph) to obtain the superconducting fraction X_{sc}, was evaluated at different temperatures from the measurement of the initial slope $\delta M/\delta H$ in the zero-field cooling regime. Since in a perfect superconductor $M = -H$, the following definition for X_{sh} was used: $X_{sh} = -\delta M/\delta H$. Low enough external fields ($H_{ext} \sim 1$ mT $\ll H_{c1}$) were applied. To take the demagnetizing factor n into account, the samples were considered to be a set of independent superconducting spheres and the field inside the superconducting fraction was taken to be $H_{ext}/(1-n)$, $n = 1/3$ (see [135] and [136] for details).

However, flux penetration between grains and the large penetration depth λ, which is close to the average grain size r, lead to flux penetration and pinning at fields below H_{c1} and to a non-linear $M(H)$ dependence. Such a non-linearity was observed in almost all $M(H)$ measurements on fullerenes [130, 132, 135–139] and makes it difficult to obtain the slope $\delta M/\delta H$ to estimate X_{sc} and to evaluate H_{c1} (see section 4). In addition, it is almost impossible to evaluate the exact magnitude of the demagnetizing factor n due to the complex geometry of the particles. Their shapes
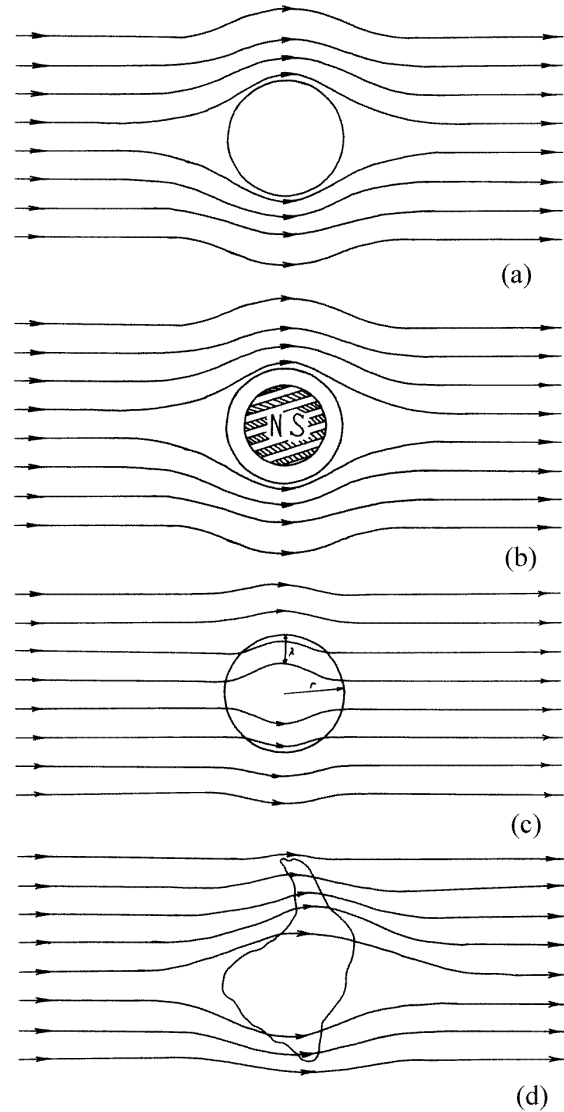

Figure 6. A schematic picture of the flux expulsion from type-II superconductors: (a) a perfect superconductor of dimension r much bigger than the penetration depth λ; (b) a sample in the normal state with a superconducting surface layer; (c) a perfect superconductor of dimension r, which is of the order of the penetration depth λ; (d) a non-ideal geometry.

are extremely irregular and the real dimensions are not well known.

From the above, it is clear that a quantitative evaluation of X_{sc} is difficult for powdered samples and should be done very carefully. Almost all of the superconducting volume fractions published for fullerene superconductors were obtained from ZFC measurements. They vary between 40 and 90% in powder samples [104, 106, 138–141]. We believe that these values should be treated as a lower limit because of granularity effects.

4. Critical fields and characteristic lengths

As mentioned in the previous chapter, two fields, the lower critical field, H_{c1}, and the upper critical field, H_{c2}, are important for the characterization of a superconductor. Both fields can be determined from magnetization measurements. In order to evaluate the parameters, which are commonly used to characterize the mixed state of type-II superconductors, the Ginzburg–Landau relations [142] can be applied:

$$\mu_0 H_{c2} = \frac{\Phi_0}{2\pi \xi^2} \qquad (1)$$

$$\mu_0 H_{c1} = \frac{\Phi_0}{4\pi \lambda^2} \ln \kappa \qquad (2)$$

$$\kappa = \lambda/\xi \qquad (3)$$

with $\Phi_0 = h/2e = 2 \times 10^{-15}$ Wb, where Φ_0 is the flux quantum, h is Planck's constant and e is the electron charge. This approach is valid for all temperatures in the dirty limit.

4.1. Upper critical field and coherence length

A large number of experiments was performed to determine the upper critical field for crystalline [120, 126, 143–146] and powdered [112, 130–132, 134–136, 138, 147–151] fullerenes as well as for thin films [127] using different techniques such as magnetization [130–132, 136, 151], ac susceptibility [134, 148], transport [127, 150] and rf absorption [149]. Almost all measurements were made on K_3C_{60} and Rb_3C_{60} and only one result is available on each of $RbCs_2C_{60}$ [136], K_2CsC_{60}, Rb_2CsC_{60} [152] and Ba_6C_{60} [153]. Other superconducting fullerenes have not yet been characterized.

To obtain the temperature dependence of the upper critical field, $H_{c2}(T)$, from dc magnetization measurements, FC curves are usually used. The critical temperature $T_c(H)$ is determined in these experiments from the crossing point of extrapolation of the linear part of the magnetization $M(T)$ in the superconducting state on the one hand, and the small normal state magnetization on the other hand. The upper critical field is equal to the applied external field, $H_{c2} = H_{ext}$, at this temperature. As an example, $H_{c2}(T)$ obtained on a Rb_3C_{60} sample in this way [135] is shown in figure 7. At temperatures not far below T_c this dependence is linear except for fields $\mu_0 H < 1$ T, where a small 'tail' is usually observed. The nature of this tail will be discussed below.

Due to the rather large values of H_{c2} and the experimental limitations of the magnetic field window (5–8 T in SQUID magnetometers), measurements of the upper critical field are usually performed at temperatures close to the transition temperature. The extrapolation of $H_{c2}(T)$ to zero is subject to a large uncertainty and depends on the fitting scheme. The standard theory of Werthamer–Helfand–Hohenberg (WHH) [154] is usually employed. This theory predicts an $H_{c2}(T)$ dependence, which follows roughly a power law $h = 0.6(1 - t^\alpha)$, where $t = T/T_c$, $h =$
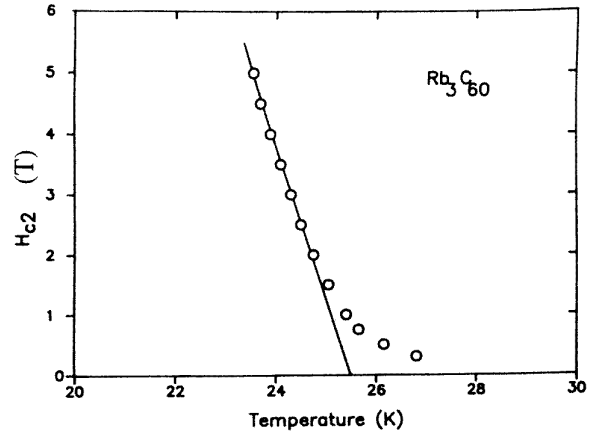

Figure 7. Upper critical field H_{c2} against temperature. The straight line corresponds to a slope $\mu_0 H' = -2.5$ T K^{-1}. (From [135]).

H/H_{c2} and $\alpha \approx 1.75$. $H_{c2}(0)$ can be evaluated from the slope, H'_{c2}, of the linear dependence near T_c by the relation

$$\mu_0 H_{c2}(0) = 0.69 T_c \left. \frac{|\mathrm{d}\mu_0 H_{c2}|}{\mathrm{d}T} \right|_{T_c}. \qquad (4)$$

In order to verify the applicability of this relation to C_{60} based materials, several experiments were performed, in which H_{c2} was measured at high magnetic fields [147–149]. Good agreement of the experimental data with the WHH prediction was obtained [147, 149], demonstrating that this theory is successful in describing fullerene superconductors (figure 8). However, Boebinger *et al* [148], who performed measurements on K_3C_{60} powder, found an enhancement of $H_{c2}(T)$ compared to theory. The authors proposed that the deviations could be attributed to flux motion in the superconducting powder, although other intrinsic mechanisms may also play a role. Additional enhancements of H_{c2} at low temperatures could result from strong electron–phonon coupling, which can lead to a relatively large increase of $H_{c2}(0)$, such that the temperature dependence of H_{c2} becomes roughly linear [155]. Fermi surface anisotropy [156] can also result in low-temperature enhancements of the upper critical field. Another mechanism proposed by the authors of [148], which we consider to be more likely, is the dirty-limit effect.

In the dirty limit, the Ginzburg–Landau coherence length ξ_{GL} is expected to be limited by the mean free path l, $\xi_{GL} \sim (\xi_0 l)^{1/2}$, where ξ_0 is the BCS coherence length. Thus, in C_{60} based superconductors, high upper critical fields might partly result from a reduction of l [148] by different types of defects. One of them could be orientational disorder between adjacent C_{60} molecules [157].

The limitation of the mean free path could be the reason for the strong scatter of the experimental data for $H_{c2}(0)$ and H'_{c2} (see table 1). For example, H'_{c2} varies for K_3C_{60} from -2 to -5.5 T K^{-1} and for Rb_3C_{60} from -2 to -3.9 T K^{-1}. This explanation could also be valid for the

Table 1. Experimentally obtained mixed state parameters of fullerene superconductors.

Compound	T_c (K)	$H_{c1}(0)$ (mT)	$H_{c2}(0)$ (T)	$-H'_{c2}$ (T K^{-1})	λ (nm)	ξ (nm)	κ
K_3C_{60}	18.5 [148]	13.2 [130]	17 [134]	1.4 [134]	240 [123]	2 [123]	92 [130]
	19 [208]	4.2 [169]	17.5 [143]	1.34 [143]	240 [130]	2.6 [130]	53 [143]
	19.3 [108]	1.2 [181]	28 [146, 147]	2 [146, 147]	240 [143]	2.9–3.3 [148]	
	19.5 [149]		30–38 [148]	2.14 [148]	480 [170]	3.4 [146, 147]	262 [181]
	19.7 [143]		38 [149]	2.18–2.8 [150]	480 [171]	4.4 [134]	
			47 [127]	2.8 [149]	600 [218]	4.5 [143]	
			49 [130]	3.5 [111]	800 [219]		
				3.73 [130]	890 [181]		
				5.5 [127]			
Rb_3C_{60}	27.5 [131]	9–11.4 [135]	40 [147]	2 [147]	320 [144]	2 [132]	80.5 [137]
	28 [98]	12 [132]	44 [135]	2.5 [135]	240–280 [135]	2.3 [135]	104–122 [135]
	29 [101, 197]	16.2 [137]	44 [134]	2.3 [134]	215 [137]	2.4 [144]	123 [132]
	29.4 [108]	3.2 [169]	46.5 [131, 221]	2.2 [221]	247 [132]	2.7 [131, 134]	
	30 [144]	1.3 [181]	62 [144]	3.28 [144]	420 [171]	3 [147]	315 [181]
			76 [149]	3.86 [149]	460 [218]		
			78 [132]	3.9 [132]	530 [220]		
					800 [219]		
					850 [181]		
$RbCs_2C_{60}$	33 [103, 136]	81 [136]	0.8 [136]	17 [136]	300 [136]	4.4 [136]	68 [136]
Ba_6C_{60}	7 [106, 153]	13 [153]	0.45 [153]	2.2 [153]	180 [153]	12 [153]	15 [153]

very small value, $H'_{c2} = -0.8$ T K^{-1}, recently obtained for $RbCs_2C_{60}$ [136].

From $H_{c2}(0)$, the coherence length ξ can be calculated using (1). Despite a large scatter (table 1), which arises from the large scatter of $H_{c2}(0)$, it is clearly seen that the coherence length of fullerene superconductors is very small (a few tens of nanometres) and comparable to the short ξ of high-T_c superconductors. According to [151] the temperature dependence of the coherence length and the penetration depth in Rb_3C_{60} can be well described by Ginzburg–Landau theory in the temperature range $0.85 < T/T_c < 1$.

One further interesting effect, that we would like to discuss here briefly, is the upturn of $H_{c2}(T)$ at temperatures very close to T_c. This upturn has been observed in almost all experiments on all superconducting compounds [130, 131, 134, 135, 138, 143, 144, 148, 152, 158]. Different authors suggested different explanations for this effect. In [130] the authors consider this deviation to be a consequence of slight variations in the local T_c, while in [134] the effect is attributed to a crossover from three to two-dimensionality. One explanation [127], less interesting from the physics point of view, is that the upturn at low fields might be due to sample imperfections. In our opinion, this explanation is not very likely because the effect has been seen in samples with superconducting fractions between 1 and 75%, i.e. under strongly varying degrees of imperfection. Buntar *et al* [146] performed detailed measurements of the upper critical field close to T_c in K_3C_{60} crystals of different quality with shielding fractions ranging from 25 to 100%. The effect was found in all samples and no influence of imperfections could be detected (figure 9). We propose that the upturn is a consequence of the anisotropy of the Fermi surface of fullerene superconductors [156]. Strong effects of the anisotropy on the magnetic properties of conventional superconductors, specifically on the $H_{c2}(T)$ dependence,

are well known [159]. The Fermi surface anisotropy exists also in fullerene superconductors in spite of their cubic lattice structure. Indeed, it was shown in [160] and [161] that an external magnetic field can lead to the appearance of Fermi surface anisotropy in metals with cubic symmetry as a consequence of a strong anisotropy of the microscopic properties. Anisotropy effects on the magnetic properties of superconducting niobium were analysed in [162] and very good agreement between theory and experiment was found.

4.2. Lower critical field and penetration depth

More than ten different methods are available for measuring H_{c1}. Some of them are listed as follows: (i) methods involving the reversible magnetization at intermediate and high external magnetic fields; (ii) the first deviation from the linear $M(H)$ behaviour; (iii) a method based on Bean's critical state model; (iv) a method based on the magnetic field dependence of λ; (v) rf methods; (vi) the torque method; (vii) the mechanical oscillator method; (viii) the μSR and EPS methods and (ix) a method involving the optical visualization of flux penetration. All of these methods require a model for the evaluation of H_{c1}. In such a situation, the reliability of the results depends substantially on how well the relationship between H_{c1} and the measured quantities can be established.

The first results on H_{c1} for K_3C_{60} [130], Rb_3C_{60} [131, 132], $RbCs_2C_{60}$ [136] and Ba_6C_{60} [153] were obtained by a dc magnetization technique. $H_{c1}(0)$ evaluated from these measurements lies in the range $\mu_0 H_{c1} = 10$–16 mT (see table 1). The temperature dependence of H_{c1} can be described well by $H_{c1}(T)/H_{c1}(0) = 1 - (T/T_c)^2$ [130] and an example of this dependence [137] is shown in figure 10. From $H_{c1}(0)$, the penetration depth λ is evaluated using (2) and the value of the coherence length known from independent measurements (subsection 4.1).
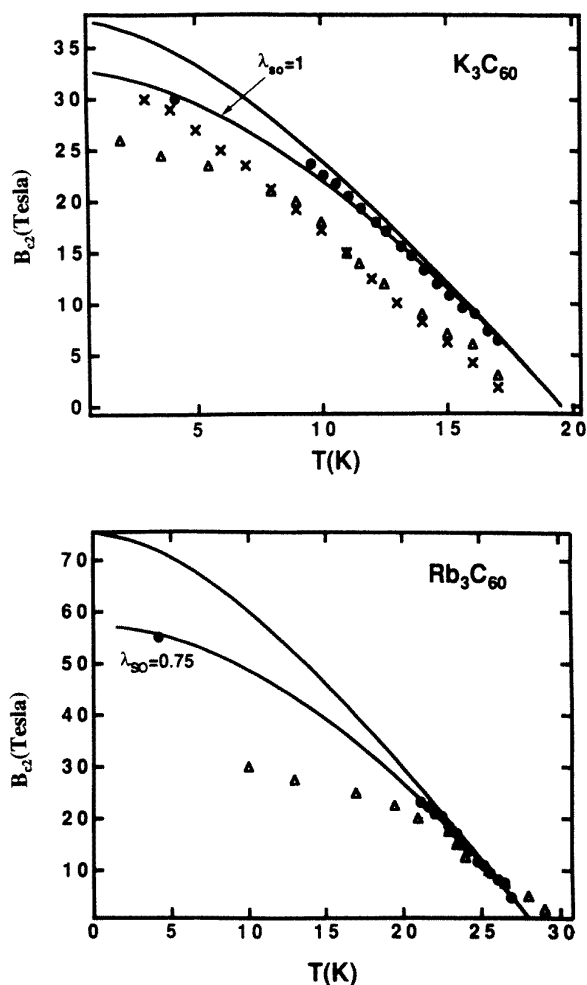
Figure 8. Upper critical field against temperature for K_3C_{60} powder and Rb_3C_{60} powder. The low-field data are taken in dc fields and the data points at 4.2 K are taken in pulsed fields. The lower solid curves are fits to the data ($\bullet$) including Pauli paramagnetic limiting and the upper curves assume no paramagnetic limiting. Both experimental dependences follow roughly the WHH prediction [154]. (After [149]).

The magnitude of λ obtained in this way is of the order of 200–250 nm (table 1).

In these experiments the lower critical field was defined as the field at which a deviation from linearity in $M(H)$ first appeared. Indeed, an ideal superconductor exhibits linear $M(H)$ behaviour up to H_{c1}, where a sharp cusp occurs. However, none of the magnetization data for fullerene materials show good linearity or any cusps. (The nature of such a behaviour is discussed in [19]). $M(H)$ usually has a smooth positive (in some experiments even a negative) curvature. It is extremely difficult to obtain the point of first deviation from such a curve, since the deviations themselves are very small.

In order to make this procedure more quantitative, it is tempting to apply Bean's critical state model [163] for the entry of vortices into hysteretic superconductors. According to this theory, the magnetization is related to
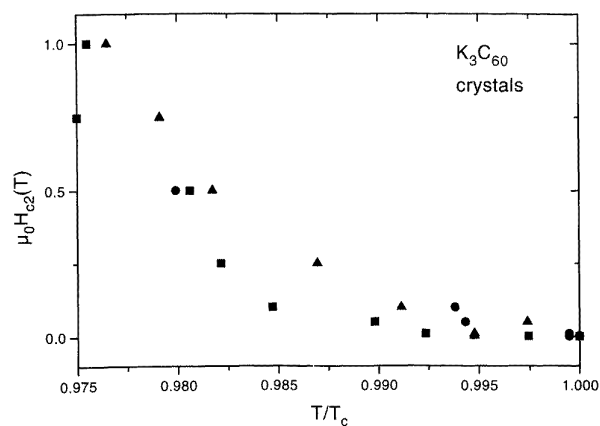

Figure 9. The temperature dependence of the upper critical field close to the transition temperature for K_3C_{60} crystals with different shielding fractions: $\bullet$, $\blacktriangle$, samples with 100% shielding; $\blacksquare$, 65% shielding.
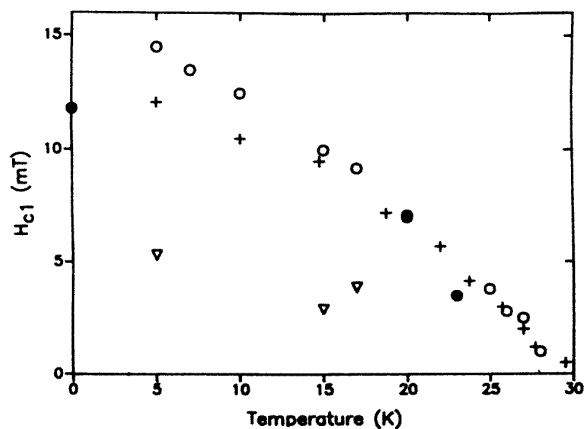

Figure 10. Lower critical field H_{c1} against temperature. $\bigcirc$, Buntar et al [137]; +, Sparn et al [132]; $\bullet$, Politis et al [135]; $\triangledown$, data obtained in [137] using Bean's critical state model. (From [137]).

the critical current density J_c (which is assumed to be field independent for simplicity), at fields above H_{c1} by $(M + H) \sim (H_a^2 - H_{c1}^2)/J_cD$, where D is a characteristic length for the sample geometry studied. This relation holds in the range $H_{c1} < H < H^*$, where $H^* \sim J_cD$ is the field at which the flux completely penetrates the sample. Thus, a plot of δM against H^2, where $\delta M = M + H_a$ is the deviation of the observed magnetization from perfect diamagnetic behaviour, should give the lower critical field. This analysis was performed for Rb_3C_{60} [137] and $RbCs_2C_{60}$ [136]. In [136] these data agreed well with the data obtained from the first deviation from a linear dependence. However, both methods led to extremely high values of H_{c1} at low temperatures and did not provide us with the 'intrinsic' values of the lower critical field. In [137] the data obtained from Bean's analysis showed much smaller values of H_{c1} (triangles in figure 10) and the authors related their data to the field at which breaking of intergranular Josephson junctions occurs.

The two above methods obviously do not lead to

satisfactory results. Therefore, Politis *et al* [135] and Buntar *et al* [136] used an analysis which is based on measurements of the reversible magnetization at high external fields and calculated H_{c1} from well known Ginzburg–Landau relations [164]:

$$-M = \frac{H_{c2}(T) - H}{(2\kappa^2 - 1)\beta_a} \qquad -M = \frac{\alpha \Phi_0}{8\pi \mu_0 \lambda^2(T)} \ln \frac{\beta H_{c2}(T)}{H}$$
(5)

for high and intermediate magnetic fields, respectively. This analysis led to lower critical fields which were slightly smaller but comparable to the data obtained by the first two methods [135, 136].

The last method, being based on direct measurements of the reversible magnetization, is more accurate for the determination of the lower critical field. However, the resulting values of the Ginzburg–Landau parameter κ and, hence, of H_{c1} strongly depend on the value of the superconducting fraction assumed (see [136], equation (4)). This leads to an enormous uncertainty in quantitative calculations, especially in the case of powdered samples with a large distribution of grain sizes.

In order to avoid the difficulties associated with the previous three methods, another way to evaluate H_{c1} must be found. In our recent investigations we used a method developed by Böhmer [165], in which H_{c1} is determined through measurements of the trapped magnetization. This method is far more accurate than the measurements of δM because of the cancellation of a large linear contribution [166]. It is based on the fact that trapped magnetic flux, M_t, can be built up in a sample only when the field has been increased beyond H_{c1}. The advantage of this method for type-II superconductors with strong pinning was illustrated in [166], where the $M(H)$ behaviour was shown to appear to be quite linear in the vicinity of H_{c1}, whereas $M_t^{1/2}$ against H showed a well resolved kink at the field corresponding to H_{c1}.

We performed such measurements on $RbCs_2C_{60}$ powder and on crystalline Rb_3C_{60} and K_3C_{60} samples. The magnetic field dependence of M_t at $T = 5$ K for a K_3C_{60} single crystal with a shielding fraction of 100% is shown in figure 11. Preliminary ac measurements indicate that there is no granularity for current flow in the sample, i.e. there should be no influence of weak links or intergranular boundaries.

As expected, at small fields, $H < H_t$, there is no trapped magnetization; M has some background value and is field independent. When the magnetic field exceeds some characteristic field H_t, a trapped magnetization appears and increases with increasing external field. The $M_t(H)$ dependence follows $M_t^{1/2} \sim H$ as predicted in [166]. The very unexpected result is that the values of H_t are very small (not higher than 1 mT at zero temperature) in comparison with those values of H_{c1} obtained previously from δM measurements. Such small values of H_t are observed for powders and crystals of different quality. Therefore, it is very unlikely that the trapped magnetization appears at small fields because of granularity or imperfections of the samples. We can certainly state that the lower critical fields of these
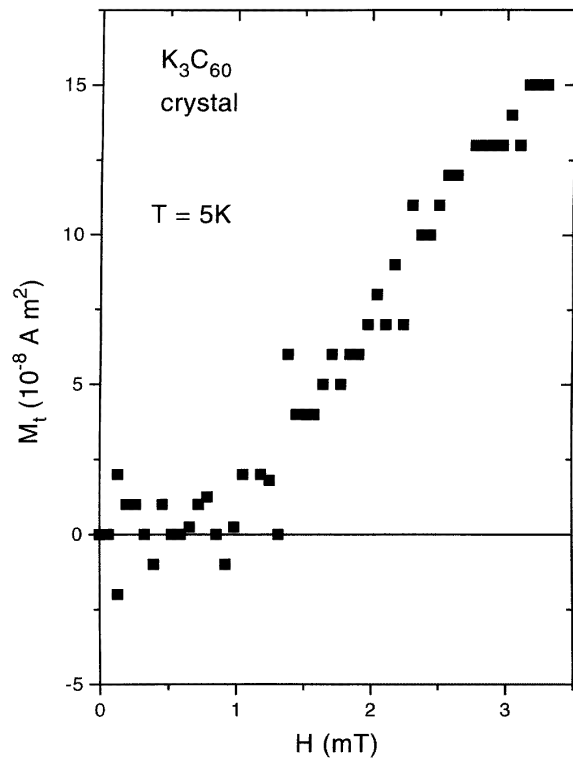

Figure 11. The magnetic field dependence of the trapped magnetization M_t at $T = 5$ K for a K_3C_{60} crystal.

fullerenes are not higher than the values of H_t observed in these experiments, because magnetic field has clearly penetrated the sample (figure 11). The smallness of H_{c1} can be explained by the fact that the electron wavefunctions between adjacent C_{60}^{3-} ions overlap relatively weakly (see subsection 2.2). This weak overlap can be easily destroyed and magnetic field starts to penetrate the sample between the C_{60} molecules.

Such small values of H_{c1} could be related to so-called molecular or zero-dimensional superconductivity in fullerenes, where the superconducting currents flow on the surface of molecules. In the case of molecular superconductivity we can hardly talk about a lower critical field and magnetic vortices penetrating the material, because any small magnetic field can easily penetrate the superconductor between the buckyballs. However, many experimental results, which are presented in this review, show that fullerenes are very strong (but conventional) type-II superconductors and that the existence of magnetic vortices describes many of the magnetic properties of these materials very well. Moreover, as we can see from $M(H)$ measurements (for instance in [131]), the magnetic field completely penetrates the sample only at fields $H_p \sim 40$ mT. This could not be the case with molecular superconductivity, because any minute field would penetrate the sample to the centre. Therefore, we consider the explanation that the smallness of H_{c1} might be due to molecular superconductivity to be unlikely.

Small values of the field at which the trapped magnetization appeared, similar to our results, were

also observed by Kraus *et al* [167], who measured the irreversible $M(T)$ curves. Additionally, in several publications small values of the penetration field were obtained [137, 168, 169], but attributed to the breaking of intergranular coupling. Moreover, in more direct measurements of λ [170, 171] by μSR experiments the penetration depth was found to be 480 nm for K_3C_{60} and 420 nm for Rb_3C_{60}, which leads to $H_{c1}(0) = 4.0$ and 4.9 mT, respectively. All of these data compel us to undertake more detailed and careful investigations of the lower critical field in fullerenes.

5. Flux pinning and related topics

Vortex lines in an ideal type-II superconductor are not fixed in the crystal lattice and their motion starts at any non-zero value of the transport current J. The movement of vortices under a Lorentz force, F_L, leads to dissipation of energy [172]. In non-ideal type-II superconductors, the vortex lines are fixed by crystal structure defects. This phenomenon is called pinning. The movement of vortices in these superconductors starts at the critical current density J_c.

The interaction between the vortex structure and the defects of the crystal structure is characterized by a force F_p per unit volume, the pinning force. The dynamical equation for a non-ideal superconductor includes the pinning force:

$$F_L + F_{tr} + F_p = [j, B] - \eta v + F_p = 0 \qquad (6)$$

where $F_{tr} = -\eta v$ is the friction force acting per unit volume of the vortex lattice, η is the viscosity coefficient and v is the velocity of the vortex line.

From a thermodynamic point of view, pinning in a type-II superconductor means that the free energy of the vortices depends on their position in the sample. The vortex lines can be pinned by different structural defects, which are called pinning centres. They can be dislocations, grain boundaries, inhomogeneities in the sample, twin boundaries etc [173].

The pinning force in a type-II superconductor is the main parameter which affects all the important superconducting properties for applications, such as the critical current density and the irreversibility line.

5.1. Critical current density

In a non-ideal type-II superconductor the vortex line begins to move when the Lorentz force F_L is strong enough to overcome the pinning force F_p. Therefore, energy dissipation appears when $F_L > F_p$. The pinning force can be written as

$$\boldsymbol{F_p} = \boldsymbol{B} \times \boldsymbol{J_c} \qquad (7)$$

where J_c is the critical current density. The strong dependence of the superconducting parameters on temperature leads to a temperature dependence of F_p. The magnetic induction determines the distance between vortices and the repulsive intervortex force is the main cause for the magnetic field dependence of F_p. All this leads to a temperature and magnetic field dependence of the critical current density.

The critical current density decreases in general monotonically with increasing T and H. The dependence $J_c(T, H)$ is linear for many superconductors in a wide range of T and H and can be well described by

$$J_c = J_0(B)\left[1 - \frac{T}{T_c(B)}\right]. \qquad (8)$$

For typical oxide superconductors $J_c(T)$ exhibits a more rapid decrease with increasing T:

$$J_c \sim J_c(0)\left[1 - \left(\frac{T}{T_c}\right)^2\right]^n \qquad (9)$$

with an exponent $n = 3$–4 (see for instance [174]).

The magnetic field dependence ($H \ll H_{c2}$) of the critical current density is often proportional to $1/B$.

All the information about the temperature and magnetic field dependence of J_c in the fullerene superconductors has been obtained from magnetization measurements. There are some specific features of the fullerenes, which cause problems with direct transport measurements on bulk samples. First of all, superconductivity is extremely unstable in air. Second, no good crystalline samples were available until very recently. Therefore, measurements of the magnetization at various magnetic fields and temperatures were performed to obtain J_c using Bean's critical state model [163]. In the simplest version of this theory, the critical current density is assumed to be field independent, which leads to a flux density distribution penetrating the sample linearly from the surface towards its centre. With increasing magnetic field, this flux gradient is pushed into the interior of the sample and reaches the centre at a certain magnetic field H^*, which manifests itself in the magnetization curve as the point where the maximum magnetization is reached. With any further increase of field, the magnetization remains unchanged. Upon decreasing the field, the sign of the flux gradient is reversed. The maximum remanent magnetization in zero field will be reached, when the field reversal takes place at $H \geq 2H^*$. Obviously, this model yields a magnetization curve which is dependent on sample size and geometry. From an experimental point of view, J_c can be determined simply from the dc magnetization curve (figure 4) by the following equation [163]:

$$J_c = A\frac{M_+ - M_-}{R}. \qquad (10)$$

In (10) A is a coefficient which is dependent on the sample geometry [163, 176], M_+ and M_- denote the magnetization measured in increasing and decreasing fields at a certain magnetic field and R is the sample radius.

The error in determining the absolute value of J_c may be large due to the uncertainty of the coefficient A and, mainly, of the sample radius R. However, the qualitative character of the temperature and magnetic field dependence is believed to be correct. Lee *et al* [177] made ac and dc magnetic measurements to evaluate J_c and showed that the dc $J_c(T)$ matched the ac results reasonably well. The authors argue that the Bean critical state model can be used for fullerene superconductors.

Table 2. Experimentally obtained superconducting parameters of fullerenes.

Compound	m (11)	J_c (A m^{-2})	$2\Delta/(k_b T_c)$	Activation energy (meV)
K_3C_{60}	1.47 [197]	10^9 [134]	3.4 [123]	33–55 [211]
	1.5 [146]	1.2×10^9 [130]	1.76 [170]	10–60 [209]
		$\sim 10^9$ [168]	3.52 [130]	
		$\sim 10^7$ [169]	5.2 [215]	
Rb_3C_{60}	1.59 [197]	10^9 [134]	3–4 [215]	33 [131]
	1.8–2 [214]	1.5×10^{10} [132]	4.1 [145]	
	2.04 [182]	2×10^{10} [151]	5.08 [213]	
		4×10^{10} [131]	7.7 [216]	
		$\sim 10^{10}$ [168]	5.4 [217]	
		$\sim 10^7$ [169]		

Some values of J_c for fullerene powders obtained in this way are shown in table 2. All these results were obtained from magnetization measurements which showed substantial hysteresis up to high enough fields. This indicates substantial flux pinning and high values of the critical current density. For instance, in Rb_3C_{60} [151] the critical current density is still 5×10^4 A cm^{-2} at 23 K and 0.5 T. It is worth mentioning that for compounds with higher critical temperature the values of J_c are higher for the same T and H. This shows indirectly that the temperature and magnetic field dependence, which we will discuss below, is similar for all fullerene compounds.

For crystalline samples, it is much more difficult to estimate the critical current density, especially for samples with a superconducting fraction below 100%. For these samples, certain assumptions about the internal microstructure must be made to obtain R. In [169], where the critical current density of crystalline K_3C_{60} and Rb_3C_{60} was investigated, J_c obtained from (10) was of the order of 10^3 A cm^{-2}, i.e. much smaller than observed earlier on powdered samples ($\sim 10^6$ A cm^{-2}). Boss *et al* [178] studied the critical current density as a function of particle size in the size range from 1 to 300 μm and found a clear linear dependence $J_c \sim 1/R$ (see table 1 in [178]). Moreover, J_c obtained for powders [131, 179] and for 1 mm sized crystals [169] is in very good agreement with this result. We presume that the 'decrease' of the critical current density with increasing sample size is caused by wrong values of R used for these calculations. The linear dependence, $J_c \sim 1/R$, means that the widths of the hysteresis loops ΔM (10) were the same for all measured samples. The real radius R of a region where the screening currents flow must be smaller than the smallest radius used for these calculations, i.e. $R < 1$ μm. This conclusion can be connected to the discussion in subsection 4.2 about molecular superconductivity in the fullerenes.

Whatever the nature of this phenomenon, it creates additional problems for J_c calculations and shows that one should be very careful with the absolute values of the critical current density evaluated from measurements of the irreversible magnetization if R is not well known. However, as we discussed before, the qualitative character of the temperature and magnetic field dependence of J_c is believed to be correct.
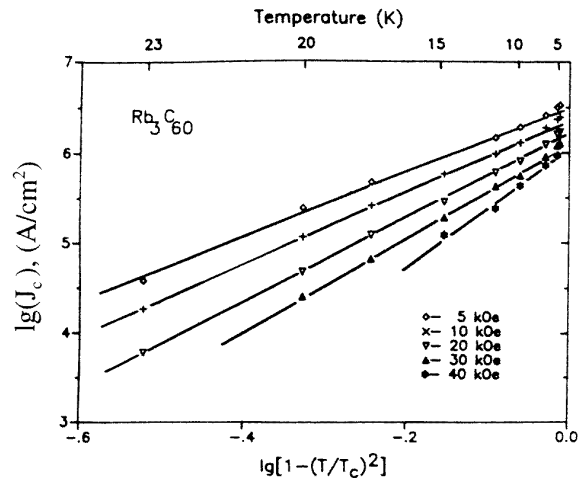

Figure 12. The double logarithmic dependence of the critical current density on $[1 - (T/T_c)^2]$ at different magnetic fields. (From [151]).

It has been shown for Rb_3C_{60} [151] and $RbCs_2C_{60}$ [180, 181] powders that the temperature dependence of J_c follows the empirical equation (9) with $n = 3$–5 for both compounds. These results are shown in figure 12. Later, similar results for K_3C_{60} powder [177, 182] and Rb_3C_{60} [177] were obtained with $n = 1.3$–5. This temperature dependence was confirmed by measurements on single-crystalline K_3C_{60} [146] and Rb_3C_{60} [169]. The higher the magnetic field, the more rapidly J_c decreases with increasing temperature.

In a wide field range, the magnetic field dependence of the critical current density of fullerenes is proportional to $1/B$, as was shown for Rb_3C_{60} [151] (see figure 13), K_3C_{60} [146] and $RbCs_2C_{60}$ [181].

5.2. The irreversibility line

An 'irreversibility temperature' was first observed by Müller *et al* [183] in LaBaCuO ceramic samples, as the point where the field cooled and the zero-field cooled curves as a function of temperature merged into one common reversible branch. This effect was then observed for all high-T_c compounds and the irreversibility line $H_{irr}(T)$,
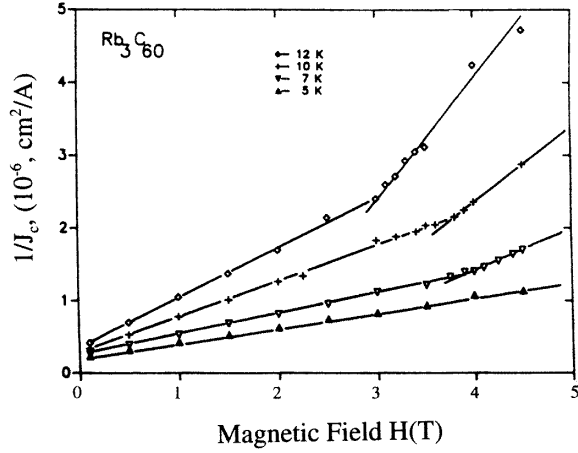
Figure 13. The magnetic field dependence of the inverse critical current density for different temperatures. (From [151]).

which separates the regions in the H–T diagram where the magnetization is reversible from the region where irreversible effects are strong, was the subject of detailed investigations. $H_{irr}(T)$ must be known for applications, because the irreversibility line indicates the values of the temperature and the magnetic field above which the critical current density is zero and the material cannot be used for current transport. From the point of view of fundamental research, $H_{irr}(T)$ provides us with important information about pinning in the sample and about structural features of the vortex system. Many experimental results show that the irreversibility line can be well described by

$$H_{irr} = H_0 \left(1 - \frac{T}{T_c}\right)^m \tag{11}$$

where H_0 is the value of H_{irr} at zero temperature. For the model of thermally activated flux motion with collective pinning [184–186], m in (11) is equal to 1.5, while for the vortex-glass models [187–189] $m = 4/3$ and for melting theories [190–196] $m = 2$.

Experimentally, the irreversibility line is usually determined from $M(T)$ measurements as the points where the ZFC and the FC curves merge (as used for K_3C_{60} and Rb_3C_{60} powders in [197]), or as the points at which the current densities drop below a certain value. For fullerenes, the irreversibility lines obtained by these methods were found to be well described by (11) with values of m between 1.47 and 2.15 (see table 2). However, the determination of the irreversibility line from the merging point of either $M(T)$ or $M(H)$ curves is as complicated as the determination of the lower critical field from the first deviation from linearity (see the discussion in subsection 4.2) and requires a certain criterion. Another method was used in [146], where $H_{irr}(T)$ was obtained as the field at which the critical current density dropped sharply to zero. In this case, a strong kink in the linear $1/J_c(H)$ dependence (11) appeared. In this work, m for the K_3C_{60} single crystal was evaluated to be 1.5.

In summary, because of the small number of experimental data, it is too early to give any final conclusions about the nature of the irreversibility line in fullerene superconductors.

5.3. Magnetic relaxation

One of the most remarkable features of some hysteretic type-II superconductors, reflecting the dynamics of flux motion, is the relaxation of the magnetization $M(t)$ at fixed temperature and magnetic field. The relaxation process has been the subject of intensive study because it heavily affects the current carrying capability of superconductors. Commonly, the relaxation is described by the flux creep activation energy U_0. The Anderson–Kim model [175] assumes a uniform barrier U_0 for the depinning of vortex bundles, resulting in a logarithmic time dependence of the magnetization:

$$M(t) = M_0 \left(1 - \frac{kT}{U_0} \ln \frac{t}{t_0}\right) \tag{12}$$

where M_0 is the unrelaxed value of M and t_0 is a time constant. Investigations of the fast relaxation in high-T_c superconductors performed by magnetic measurements demonstrated that in most cases a logarithmic dependence was indeed observed [195, 198–204]. The corresponding activation energy U_0 increases with increasing temperature [199, 200, 202–205]. Various theoretical explanations of this phenomenon in the framework of different models were put forward, such as a vortex-glass transition [187], intergranular decoupling [202], percolation of the magnetic flux in random pinning potentials [200], non-linear dependence of the pinning potential on current $U_p(j)$ [201, 206] and collective pinning [207].

Investigations of the magnetic relaxation have been also carried out on fullerene superconductors [131, 208, 209, 181]. In [131], [208] and [209] the flux creep activation energy was estimated to be of the order of 10^{-2} eV (see figure 5). However, it should be pointed out that all of these measurements were made on powder samples and that the magnetic relaxation did not follow a logarithmic dependence [208]. Even peaks were observed in $M(t)$ curves during short-term relaxation [181]. This behaviour can be connected to intergranular coupling between grains in powder samples as well as to weak links, which may exist in samples of poor quality. Very recently [210, 211] the magnetization relaxation was studied in K_3C_{60} crystals of different quality. It was shown [210] that inhomogeneities in the superconductor strongly affected the relaxation process, which might mask the logarithmic $M(t)$ dependence, which for samples of good quality the magnetic relaxation followed the $M \sim \ln(t)$ behaviour, as shown in figure 14. It was also observed [211] that the flux creep rate increased progressively with temperature, up to at least $T = 17$ K $\cong 0.88T_c$, and that the temperature dependence of the flux creep activation energy showed a peak at some characteristic temperature T_p (figure 15), which had a roughly linear field dependence $T_p(H)$. The values of the flux creep activation energy varied in the range $U_0 = 10$–80 meV and are similar to those obtained in oxide superconductors.
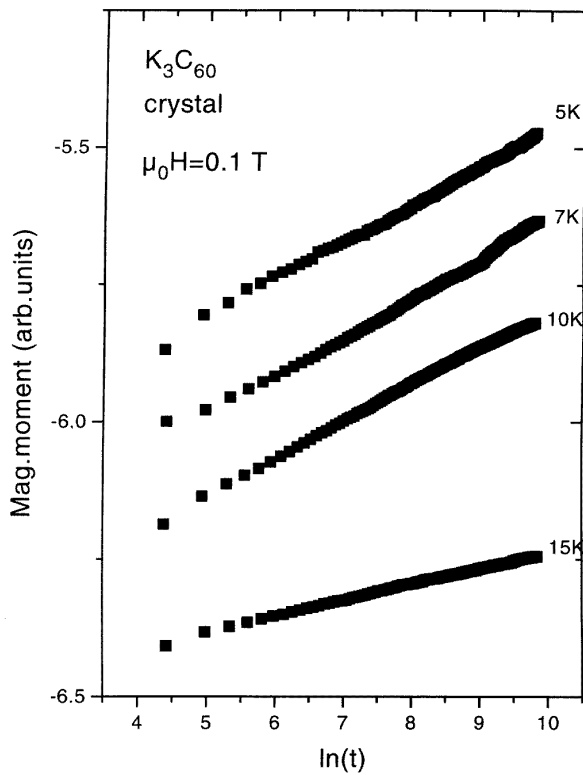
Figure 14. Decay of the remanent magnetization M with $\ln t$ at different temperatures.
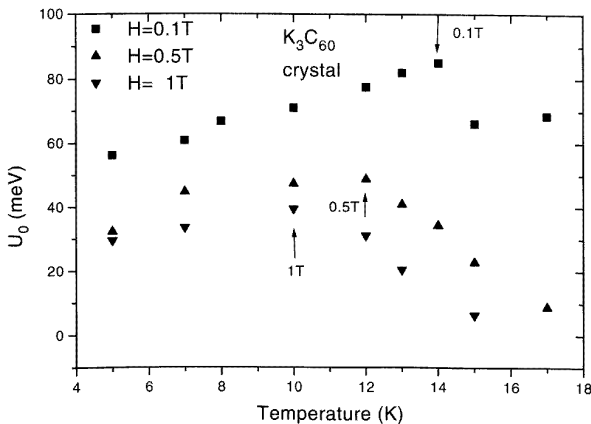

Figure 15. The temperature dependence of the flux creep activation energy for a K_3C_{60} single crystal.

Additional investigations of the magnetic relaxation will have to be done on samples of good quality and on different compounds, in order to establish the relaxation mechanisms.

5.4. Pinning problems

As was shown in the previous sections, there is good evidence that flux lines penetrate the fullerene superconductors. Because of the three-dimensional structure of the fullerene superconductors, these lines should build up an Abrikosov vortex lattice. As we

discussed before, vortices are pinned on pinning centres in the presence of different structural defects in the material. Information on what kinds of structural defect act as better pinning centres and on the strength of the pinning force produced by these defects is very important both from the fundamental point of view and for the applicability of these materials. However, nothing is known about structural defects in fullerene superconductors so far and, therefore, we do not have any information about pinning of magnetic flux in these substances. The only point we can make is that pinning in fullerenes is strong, based on the large hysteresis of the $M(H)$ dependence and the large differences between the ZFC and the FC curves.

New research has to be performed on samples of good quality with known structural features and structural defects to provide us with this very important information on the fullerene superconductors.

6. Conclusions

In the present contribution, an attempt has been made to highlight some experimental results on the magnetization of crystalline and powdered fullerene superconductors and to emphasize the role of these experiments in achieving an improved insight into the physics of fullerene superconductivity.

Our discussion of experimental results deduced from magnetic measurements may be summarized as follows.

Only two superconducting fullerenes, K_3C_{60} and Rb_3C_{60}, have been characterized by several groups. Only one measurement of the critical fields and the characteristic lengths has been performed for the compounds $RbCs_2C_{60}$ [136], Ba_6C_{60} [153] and sodium doped C_{60} [138]. No other fullerene superconductors have yet been characterized.

The values of H_{c2} vary widely from sample to sample, while the values of H_{c1} cannot be compared because only one or two data points exist for each compound as mentioned in subsection 4.2. Moreover, the values of H_{c1} deduced from these experiments seem to be overestimated.

Measurements of the temperature and magnetic field dependence of the magnetization show that pinning is very strong in fullerenes. However, the nature of flux pinning is unclear at present and we do not know whether strong pinning is an intrinsic property of the C_{60} molecules or extrinsic and caused by different defects in the alkali metal doped C_{60} lattice.

In conclusion, we wish to point out that the effects of granularity in powdered samples and the possible granularity of bulk crystals represent a central problem at present, because one needs to know whether the parameters obtained from experiment are characteristic of the bulk material or of weak links, in order to establish the intrinsic superconducting parameters of these new superconductors. We believe that with the increasing quality of single crystals, significant progress towards a better understanding of the mixed state properties lies immediately ahead, and that magnetization measurements and their comparison with other techniques will play a key role in this development.

Acknowledgments

References

[1] Kroto H W, Heath J R, O'Brien S C, Curl R F and Smalley R E 1985 *Nature* **318** 162
[2] 1992 *Accounts Chem. Res.* **25**
[3] 1992 *J. Phys. Chem. Solids* **53** No 12
[4] 1992 *Carbon* **8** No 8
[5] 1993 *J. Phys. Chem. Solids* **54** No 12
[6] 1994 *MRS Bull.* **19** No 11
[7] Hirsh A 1993 *The Chemistry of Fullerenes* (Berlin: Thieme)
[8] Baggot J 1994 *Perfect Symmetry: The Accidental Discovery of a New Form of Carbon* (Oxford: Oxford University Press)
[9] Weltner W Jr and Van Zee R J 1989 *Chem. Rev.* **89** 1713
[10] Curl R F and Smalley R E 1991 *Sci. Am.* **October** 32
[11] Kroto H W, Allaf A W and Balm S P 1991 *Chem. Rev.* **91** 1213
[12] Diederich F and Rubin Y 1992 *Angew. Chem. Int. Edn Engl.* **31** 1101
[13] Hebard A F 1993 *Annu. Rev. Mater. Sci.* **23** 159
[14] Fischer J E and Heiney P A 1993 *J. Phys. Chem. Solids* **54** 1725
[15] Weaver J H and Poirier D M 1994 *Solid State Physics* vol 48, ed H Ehrenreich and F S Paepen (New York: Academic)
[16] Meingast C and Gugenberger F 1993 *Mod. Phys. Lett.* B **7** 1703
[17] Ogata H *et al* 1993 *Mod. Phys. Lett.* B **7** 1173
[18] Hebard A F 1992 *Phys. Today* **45** 26
[19] Ramirez A P 1994 *Supercond. Rev.* **1** 1
[20] Gelfand M P 1994 *Supercond. Rev.* **1** 103
[21] Dresselhaus M S, Dresselhaus G and Saito R 1994 *Physical Properties of High Temperature Superconductors IV* ed D M Ginsberg (Singapore: World Scientific) p 471
[22] Buntar V 1995 *Recent Advances in the Chemistry and Physics of Fullerenes and Related Materials II* ed K M Kadish and R S Ruoff (Pennington, NJ: ECS) p 994
[23] Rohlfing E A, Cox D M and Kaldor A 1984 *J. Chem. Phys.* **81** 3322
[24] Krätschmer W, Lamb L D, Fostiropoulos K and Huffman D R 1990 *Nature* **347** 345
[25] Heiney P A 1992 *J. Phys. Chem. Solids* **53** 1333
[26] Prassides K, Kroto H W, Taylor R, Walton D R M, David W I B, Tomkinson J, Haddon R C, Rosseinsky M J and Murphy D W 1993 *Carbon* **30** 1277
[27] Fleming R M *et al* 1991 *Mater. Res. Soc. Symp. Proc.* vol 206, ed R S Averback, J Bernholc and D L Nelson (Pittsburg, PA: Materials Research Society)
[28] Heiney P A, Fischer J E, McGhie A R, Romanow W J, Denenstein A M, McCauley J P and Smith A B III 1991 *Phys. Rev. Lett.* **66** 2911
[29] Sachidanadan R A and Harris A B 1991 *Phys. Rev. Lett.* **67** 1467
[30] Dworkin A, Szware H, Leach S, Hare J P, Dennis T J, Kroto H W, Taylor R and Walton D R M 1991 *C.R. Acad. Sci. Paris* II **312** 979
[31] David W I F, Ibberson R M, Dennis T J S, Hare J P and Prassides K 1992 *Europhys. Lett.* **18** 219
[32] David W I F, Ibberson R M, Dennis T J S, Hare J P and Prassides K 1992 *Europhys. Lett.* **18** 735
[33] Yu R C, Tea N, Salamon M B, Lorents D and Malhotra R 1992 *Phys. Rev. Lett.* **68** 2050
[34] Zubov V I, Tretiakov N P, Teixeira Rabelo J N and Sanches Ortiz J F 1994 *Phys. Lett.* **194A** 223
[35] Zubov V I, Tretiakov N P, Teixeira Rabelo J N and Sanches Ortiz J F 1995 *Mater. Res. Soc. Symp. Proc.* vol 359 (Pittsburgh, PA: Materials Research Society) p 253
[36] Haddon R C and Elser V 1990 *Chem. Phys. Lett.* **169** 362
[37] Ruoff R S, Beach D, Cuomo J, McGuire T, Whetten R L and Diederich F 1991 *J. Phys. Chem. Solids* **95** 3457
[38] Haddon R C, Schneemeyer L F, Waszczak J V *et al* 1991 *Nature* **350** 46
[39] Haddon R C and Pasquarello A 1994 *Phys. Rev.* B **50** 16459
[40] Ramirez A P, Haddon R C, Zhou O *et al* 1994 *Science* **265** 84
[41] Allemand P, Khemani M C, Koch A *et al* 1991 *Science* **253** 301
[42] Wudl F and Thompson J D 1992 *J. Phys. Chem. Solids* **53** 1449
[43] Sparn G *et al* 1992 *Solid State Commun.* **82** 779
[44] Schilder A *et al* 1994 *Phys. Rev. Lett.* **73** 1299
[45] Tanaka K *et al* 1993 *Phys. Rev.* B **47** 7554
[46] Cevc P *et al* 1994 *Europhys. Lett.* **26** 707
[47] Venturini P *et al* 1992 *Int. J. Mod. Phys.* B **23** 3947
[48] Reshadri R *et al* 1993 *Solid State Commun.* **85** 971
[49] Lappas A, Prassides K *et al* 1995 *Science* **267** 1799
[50] Gotschy B 1995 *Phys. Rev.* B **52** 7378
[51] Völkel G *et al* 1995 *Phys. Rev.* B **52** 10 188
[52] Arovas D P and Auerbach A 1995 *Phys. Rev.* B **52** 10 114
[53] Ricco M, Cristofolini L, De Renzi R *et al* 1995 *Physics and Chemistry of Fullerenes and Derivatives* ed H Kuzmany (Singapore: World Scientific)
[54] Wang Y 1992 *Nature* **356** 585
[55] Flom S R, Pong R G, Bartoli F J and Kafafi Z H 1992 *Phys. Rev.* B **46** 15 598
[56] Lu J P, Li X-P and Martin R M 1992 *Phys. Rev. Lett.* **68** 1551
[57] Shi X D, Kortan A R, Williams J M, Kini A M, Savall B M and Chaikin P M 1992 *Phys. Rev. Lett.* **68** 827
[58] Alers G B *et al* 1992 *Science* **257** 511
[59] Gugenberger F *et al* 1992 *Phys. Rev. Lett.* **69** 3774
[60] Grivei E, Nysten B, Cassart M *et al* 1993 *Phys. Rev.* B **47** 1705
[61] Matsuo T *et al* 1992 *Solid State Commun.* **83** 711
[62] Buntar V, Weber H W and Ricco M 1995 *Solid State Commun.* **98** 175
[63] Song L W *et al* 1993 *Solid State Commun.* **87** 387
[64] Grigoryan L and Tokumoto M 1995 *Solid State Commun.* **96** 523
[65] Grushko Yu private communication
[66] Vaughan G B M *et al* 1991 *Science* **254** 1350
[67] Fleming R M *et al* 1991 *Phys. Rev.* B **44** 888
[68] Verheijen M A *et al* 1992 *Chem. Phys.* **166** 287
[69] Tendeloo G V *et al* 1993 *Europhys. Lett.* **21** 329
[70] Mitsuki T *et al* 1994 *Japan. J. Appl. Phys.* **33** 6281
[71] Tomita M *et al* 1992 *Appl. Phys. Lett.* **61** 1171
[72] Oh D-H and Hee Lee Y 1995 *Phys. Rev. Lett.* **75** 4230
[73] Christides C *et al* 1993 *Europhys. Lett.* **22** 611
[74] Winter J and Kuzmany H 1992 *Solid State Commun.* **84** 935
[75] Zhu Q, Zhou O, Bykovetz N, Fischer J E *et al* 1993 *Phys. Rev.* B **47** 13 948
[76] Tycko T, Dabbagh G *et al* 1993 *Phys. Rev.* B **48** 9097
[77] Chauvet O, Oszlanyi S, Forro L *et al* 1994 *Phys. Rev.*

Lett. **72** 2721

[78] Pekket S, Forro L, Mihaly L *et al* 1994 *Solid State Commun.* **90** 349

[79] Stephens P W, Bortel G, Faigel G *et al* 1994 *Nature* **370** 636

[80] Pekket S, Janossy A, Mihaly L *et al* 1994 *Science* **265** 1077

[81] Rao A M *et al* 1993 *Science* **259** 955

[82] Robert J *et al* 1995 *Solid State Commun.* **96** 143

[83] Uemura Y *et al* 1995 *Phys. Rev.* B **52** R6991

[84] Macfarlane W *et al* 1995 *Phys. Rev.* B **52** R6995

[85] Cristofolini L *et al* 1995 *J. Phys.: Condens. Matter* **7** L567

[86] Hariyaga K 1996 *Phys. Rev.* B **53** R4197

[87] Bommeli F *et al* 1995 *Phys. Rev.* B **51** 20

[88] Janossy A, Chauvet O *et al* 1993 *Phys. Rev. Lett.* **71** 1091

[89] Martin M C, Koller D, Rosenberg A *et al* 1995 *Phys. Rev.* B **51** 3210

[90] Zhu Q, Cox D E and Fischer J E 1995 *Phys. Rev.* B **51** 3966

[91] Oszlany G *et al* 1995 *Phys. Rev.* B **51** 12 228

[92] Granasy L *et al* 1996 *Solid State Commun.* **97** 573

[93] Kosaka M *et al* 1995 *Phys. Rev.* B **51** 12 018

[94] Lappas A *et al* 1995 *J. Am Chem. Soc.* **117** 7560

[95] Hannay N B, Geballe T H, Matthias B T, Geballe T H, Anders K, Schmidt P and Macnair D 1965 *Phys. Rev. Lett.* **14** 225

[96] Hadon R C *et al* 1991 *Nature* **350** 320

[97] Hebard A F, Rosseinsky M J, Haddon R C, Murphy D W, Glarum S H, Palstra T T M, Ramirez A P and Kortan A R 1991 *Nature* **350** 600

[98] Rosseinsky M J, Ramirez A P, Glarum S H, Murphy D W, Haddon R C, Hebard A F, Palstra T T M, Kortan A R, Zahurak S M and Makhija A V 1991 *Phys. Rev. Lett.* **66** 2830

[99] Bednorz J G and Müller K A 1986 *Z. Phys.* B **64** 189

[100] Chu C W, Hor P H, Meng R L *et al* 1987 *Phys. Rev. Lett.* **58** 405

[101] Tanigaki K, Hirosawa I, Ebbesen T W, Mizuki J, Shimakawa Y, Kubo Y, Tsai J S and Kuroshima S 1992 *Nature* **356** 419

[102] Palstra T T M, Zhou O, Iwasa Y, Sulewski P E, Fleming R M and Zegarski B R 1995 *Solid State Commun.* **93** 327

[103] Tanigaki K, Hirosawa I, Ebbesen T W, Mizuki J-I and Tsai J-S 1993 *J. Phys. Chem. Solids* **54** 1645

[104] Stephens P W, Mihaly L, Lee P L, Whetten R L, Huang S-M, Kaner R, Diederich F and Holtzer K 1991 *Nature* **351** 632

[105] Kortan A R, Kopylov N, Glarum S, Gyorgy E M, Ramirez A P, Fleming R M, Thiel F A and Haddon R C 1992 *Nature* **355** 529

[106] Kortan A R, Kopylov N, Glarum S, Gyorgy E M, Ramirez A P, Fleming R M, Zhou O, Thiel F A, Trevor P L and Haddon R C 1992 *Nature* **360** 566

[107] Kraus M, Kanovski M, Baenitz M, Werner H, Schlögl R, Scheidt E-W, Vieth H-M and Lüders K 1995 *Fullerene Sci. Technol.* **3** 115

[108] Fleming R M, Ramirez A P, Rosseinsky M K, Murphy D W, Haddon R C, Zahurak S M and Makhija A V 1991 *Nature* **352** 787

[109] Zhou O *et al* 1992 *Science* **255** 833

[110] Oshiyama A and Saito S 1992 *Solid State Commun.* **82** 41

[111] Ramirez A P, Rosseinsky M J, Murphy D W and Haddon R C 1992 *Phys. Rev. Lett.* **69** 1687

[112] Tyco R *et al* 1991 *Science* **253** 884

[113] Schirber J E *et al* 1993 *J. Phys. Chem. Solids* **54** 1427

[114] Kniaz J, Fischer J E, Zhu Q, Rosseinsky M K, Zhou O and Murphy D W 1993 *Solid State Commun.* **88** 47

[115] Prassides K, Christides C, Thomas I M, Mizuki J, Tanigaki K, Hirosawa I and Ebbesen T W 1994 *Science* **263** 950

[116] Yildirim T, Fischer J E, Dinnebier R, Stephens P W and Lin C L 1995 *Solid State Commun.* **93** 269

[117] Yildirim T, Fischer J E, Harris A B, Stephans P W, Liu D, Brard L, Strongin R M and Smith A B III 1993 *Phys. Rev. Lett.* **71** 1383

[118] Kochanski G P, Hebard A F, Haddon R C and Fiory A T 1992 *Science* **255** 184

[119] Stepniak F, Benning P J, Poirier D M and Weaver J H 1993 *Phys. Rev.* B **48** 1899

[120] Xiang X-D, Hou J G, Briceno G, Vareka W A, Mostovoy R, Zettl A, Crespi V H and Cohen M L 1992 *Science* **256** 1190

[121] Hebard A F, Palstra T T M, Haddon R C and Fleming R M 1993 *Phys. Rev.* B **48** 9945

[122] Vareka W A, Fuhrer M S and Zettl A 1994 *Physica* C **235–240** 2507

[123] Wong W H *et al* 1992 *Europhys. Lett.* **18** 79

[124] Hou J G, Lu L, Crespi V H, Xiang X-D, Zettl A and Cohen M L 1995 *Solid State Commun.* **93** 973

[125] Lee M W, Tai M F, Luo S C and Shi J B 1995 *Physica* C **245** 6

[126] Ogata H, Inabe T, Hoshi H, Maruyama Y, Achiba Y, Suzuki S, Kikuchi K and Ikemoto I 1992 *Japan. J. Appl. Phys.* **31** L166

[127] Palstra T T M, Haddon R C, Hebard A F and Zaanen J 1992 *Phys. Rev. Lett.* **68** 1054

[128] Quirion G *et al* 1993 *Europhys. Lett.* **21** 233

[129] Yan D and Li W 1995 *Phys. Lett.* **208A** 335

[130] Holczer K, Klein O, Grüner G, Thompson J D, Diederich F and Whetten R L 1991 *Phys. Rev. Lett.* **67** 271

[131] Politis C, Buntar V, Krauss W and Gurevich A 1992 *Europhys. Lett.* **17** 175

[132] Sparn G, Thompson J D, Whetten R L, Huang S-M, Kaner R B, Diederich F, Grüner G and Holtzer K 1992 *Phys. Rev. Lett.* **68** 1228

[133] Sokolov A I, Kufaev Yu A and Sonin E B 1993 *Physica* C **212** 19

[134] Baenitz M, Heinze M, Straube E, Werner H, Schlögl R, Thommen V, Güntherodt H-J and Lüders K 1994 *Physica* C **228** 181

[135] Politis C, Sokolov A I and Buntar V 1992 *Mod. Phys. Lett.* B **6** 351

[136] Buntar V, Ricco M, Cristofolini L, Weber H W and Bolzoni F 1995 *Phys. Rev.* B **52** 4432

[137] Buntar V, Eckern U and Politis C 1992 *Mod. Phys. Lett.* B **6** 1037

[138] Khairullin I I, Imaeda K, Yakushi K and Inokuchi H 1994 *Physica* C **231** 26

[139] Stenger V A, Pennington C H, Buffinger D R and Ziebarth R P 1995 Nuclear magnetic resonance of A_3C_{60} superconductors *Preprint*

[140] Tokumoto M, Tanaka Y, Kinoshita N, Kinoshita T, Ishibashi S and Ihara H 1993 *J. Phys. Chem. Solids* **54** 1667

[141] Imaeda K, Khairullin I I, Yakushi K and Inokuchi H *Proc. ICSM'94 (Seoul 1994); Synth. Met.* at press

[142] deGennes P G 1966 *Superconductivity of Metals and Alloys* (New York: Benjamin)

[143] Hou J G, Crespi V H, Xiang X-D, Vareka W A, Briceno G, Zettl A and Cohen M L 1993 *Solid State Commun.* **86** 643

[144] Hou J G, Xiang X-D, Crespi V H, Cohen M L and Zettl A 1994 *Physica* C **228** 175

[145] Gu C *et al* 1994 *Phys. Rev.* B **50** 16 566

[146] Buntar V, Sauerzopf F M, Weber H W and Fischer J E 1996 *Recent Advances in Chemistry and Physics of Fullerenes and Related Materials* vol 3 at press

[147] Johnson C E, Jiang H W, Holtczer K, Kaner R B, Whetten R L and Diederich F 1992 *Phys. Rev.* B **46** 5880

[148] Boebinger G S, Palstra T T M, Passner A, Rosseinsky M J and Murphy D W 1992 *Phys. Rev.* B **46** 5876

[149] Foner S, McNiff E J, Heiman D, Huang S-M and Kaner

R B 1992 *Phys. Rev.* B **46** 14 936

[150] Hou J G, Xiang X-D, Cohen M L and Zettl A 1994 *Physica* C **232** 22

[151] Politis C, Buntar V and Seminozhenko V P 1993 *Int. J. Mod. Phys.* B **7** 2163

[152] Baenitz M, Heinze M, Lüders K, Werner H and Schlögl R *Proc. IWEP'95 (Kirchberg, 1995)* (Singapore: World Scientific) at press

[153] Korenivski V, Rao K V and Iqbal Z 1994 *Phys. Rev.* B **50** 13 890

[154] Werthamer N R, Helfand E and Hohenberg P C 1966 *Phys. Rev.* **147** 295

[155] Carbotte J P 1990 *Rev. Mod. Phys.* **62** 1027

[156] Erwin S C and Pickett W E 1991 *Science* **254** 842

[157] Gelfand M P and Lu J P 1992 *Phys. Rev. Lett.* **68** 1050

[158] Baenitz M, Heinze M, Lüders K, Werner H and Schlögl R 1994 *Solid State Commun.* **91** 337

[159] Weber H W (ed) 1977 *Anisotropy Effects in Superconductors* (New York: Plenum) p 316

[160] Marchenkov V V, Cherepanov A N, Startsev V E, Czurda C and Weber H W 1995 *J. Low. Temp. Phys.* **98** 425

[161] Marchenkov V V, Weber H W, Cherepanov A N and Startsev V E 1996 *J. Low. Temp. Phys.* **102** 133

[162] Weber H W, Seidl E, Laa C, Schachinger E, Prohammer M, Junod A and Eckert D 1991 *Phys. Rev.* B **44** 7585

[163] Bean C P 1962 *Phys. Rev. Lett.* **8** 250

[164] Abrikosov A A 1957 *Zh. Eksp. Teor. Fiz.* **32** 1442

[165] Böhmer C 1995 *PhD Thesis* Technical University, Vienna

[166] Moshchalkov V, Henry J V, Marin C, Rossat-Mignod J and Jacquot J F 1991 *Physica* C **175** 407

[167] Kraus M, Sindlinger H, Werner H, Schlögl R, Thommen V, Lang H P, Gütherodt H-J and Lüders K 1995 *Proc. 8th ISIC (Vancouver, 1995)*; *J. Phys. Chem. Solids*

[168] Thompson J D, Sparn G, Holczer K, Klein O, Grüner G, Kaner R B, Diederich F and Whetten R L 1994 *Physical and Material Properties of High Temperature Superconductors* ed S K Malic and S S Shah (Commack, NJ: Nova) p 139

[169] Irons S H, Liu J Z, Klavins P and Shelton R N 1995 *Phys. Rev.* B **52** 15 517

[170] Uemura Y J *et al* 1991 *Nature* **352** 606

[171] Uemura Y J, Keren A, Le L P *et al* 1994 *Physica* C **235–240** 2501

[172] Gurevich A V, Minz R G and Rakhmanov A L 1987 *Physics of Composed Conductors* (Moscow: Nauka) p 240

[173] Campbell A M and Evetts J E (ed) 1972 *Critical Currents in Superconductors* (London: Taylor and Francis)

[174] Matsushita T, Otabe E S, Ni B *et al* 1991 *Japan. J. Appl. Phys.* **30** L342

[175] Anderson P W and Kim Y B 1964 *Rev. Mod. Phys.* **36** 39

[176] Fietz W A and Webb W W 1969 *Phys. Rev.* **178** 657

[177] Lee M W, Tai M F, Luo S C and Shi J B 1995 *Physica* C **245** 6

[178] Boss R D, Briggs J S, Jacobs E W, Jones T E and Mosier-Boss P A 1995 *Physica* C **243** 29

[179] Buntar V and Politis C 1993 *Meeting Mater. Res. Soc. (Boston, MA, 1993)*

[180] Buntar V, Ricco M, Cristofolini L, Grassi M and Bolzoni F 1995 *Physics and Chemistry of Fullerenes and Derivatives* ed H Kuzmany, J Fink, M Mehring and S Roth (Singapore: World Scientific) p 440

[181] Buntar V *et al* to be published

[182] Tai M F, Chang G F and Lee M W 1995 *Phys. Rev.* B **52** 1176

[183] Müller K A, Takashige M and Bednorz J G 1987 *Phys. Rev. Lett.* **58** 1143

[184] Yeshurun Y and Malosemoff A P 1988 *Phys. Rev. Lett.* **60** 2202

[185] Tinkham M 1988 *Phys. Rev. Lett.* **61** 1658

[186] Hagen C W and Griessen R 1989 *Phys. Rev. Lett.* **62** 2857

[187] Fisher D S, Fisher M P A and Huse D A 1991 *Phys. Rev.* B **43** 130

[188] Gammel P L *et al* 1991 *Phys. Rev. Lett.* **66** 953

[189] Koch R H *et al* 1989 *Phys. Rev. Lett.* **63** 1511

[190] Houghton A, Pelcovits R A and Sudbø A 1989 *Phys. Rev.* B **40** 6763

[191] Brandt E H 1989 *Phys. Rev. Lett.* **63** 1106

[192] Farrel D E, Rice J P and Ginsberg D M 1991 *Phys. Rev. Lett.* **67** 1165

[193] Beck R G *et al* 1992 *Phys. Rev. Lett.* **68** 1594

[194] Glazman L I and Koshelev A E 1991 *Phys. Rev.* B **43** 2835

[195] Schmidt M F, Israeloff N E and Goldman A M 1993 *Phys. Rev. Lett.* **70** 2162

[196] Blatter G and Ivlev B 1993 *Phys. Rev. Lett.* **70** 2621

[197] Lin C L, Mihalisin T, Bykovetz N, Zhu Q and Fischer J E 1994 *Phys. Rev.* B **49** 4285

[198] Gurevich A and Küpfer H 1993 *Phys. Rev.* B **48** 6477

[199] Campbell I A, Fruchter L and Cabanel R 1990 *Phys. Rev. Lett.* **64** 1561

[200] Gurevich A, Küpfer H and Keller C 1991 *Europhys. Lett.* **15** 789

[201] Maley M P, Willis J O, Lessure H and McHenry M E 1990 *Phys. Rev.* B **42** 2639

[202] Keller C, Küpfer H, Gurevich A *et al* 1990 *J. Appl. Phys.* **68** 3498

[203] Xue Y Y, Huang Z J, Fang H H *et al* 1992 *Physica* C **194** 194

[204] Xu Y *et al* 1989 *Phys. Rev.* B **40** 10 882

[205] Sun Y R, Thompson J R, Christen D K *et al* 1992 *Physica* C **194** 403

[206] Sun J Z, Eom C B, Lairson B *et al* 1991 *Phys. Rev.* B **43** 3002

[207] Yamafuji K *et al* 1989 *Physica* C **159** 743

[208] Lin C L, Mihalisin T, Labes M M, Bykovetz N, Zhu Q and Fischer J E 1994 *Solid State Commun.* **90** 629

[209] Lee M W, Tai M F and Luo S C 1995 *Japan. J. Appl. Phys.* **34** 126

[210] Buntar V, Sauerzopf F M, Weber H W, Fischer J E, Kuzmany H, Haluska M and Lin C L 1996 *Recent Advances in Chemistry and Physics of Fullerenes and Related Materials* vol 3 at press

[211] Buntar V, Sauerzopf F M, Weber H W, Fischer J E, Kuzmany H, Haluska M and Lin C L to be published

[212] Mizuki J *et al* 1994 *Phys. Rev.* B **50** 3466

[213] Gupta R P 1994 *Physica* C **235–240** 2497

[214] Warden M, Schauwecker R, Erhart P, Ivanshin V A *et al* 1994 *Physica* C **235–240** 2505

[215] Tycko R *et al* 1992 *Phys. Rev. Lett.* **68** 1912

[216] Els G *et al* 1994 *Physica* C **235–240** 2475

[217] Jess P *et al* 1994 *Physica* C **235–240** 2499

[218] Tycko R *et al* 1992 *Phys. Rev. Lett.* **68** 1912

[219] Degiorgi L *et al* 1992 *Phys. Rev. Lett.* **69** 2987

[220] Sakamoto N *et al* 1995 *Japan. J. Appl. Phys.* **34** L1267

[221] Heinze M *et al* 1996 *Synth. Met.* **77** 23